ILMATIETEEN LAITOS
METEOROLOGISKA INSTITUTET
FINNISH METEOROLOGICAL INSTITUTE

151
CONTRIBUTIONS

MICROWAVE REMOTE SENSING OF SNOW AND ENVIRONMENT

MATIAS TAKALA

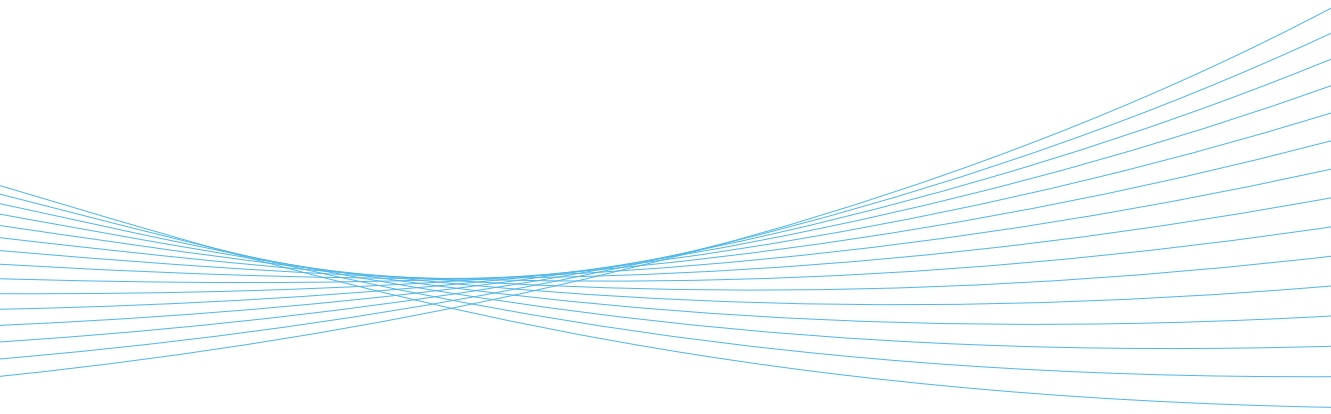

ILMATIETEEN LAITOS

		Julkaisun sarja, numero ja raporttikoodi
Julkaisija	Ilmatieteen laitos (Erik Palménin aukio 1) PL 503, 00101 Helsinki	FMI Contributions 151 Joulukuu 2018

Tekijä(t)

Takala, Matias

Nimeke Lumen ja ympäristön mikroaaltokaukokartoitus

Tiivistelmä

Pohjoisen pallonpuoliskon lumialueen laajuus ja lumen massa ovat kaksi tärkeää fysikaalista parametria, jotka vaikuttavat veden ja hiilen kiertoon sekä säteilytasapainoon erityisesti korkeilla leveysasteilla. Tässä väitöksessä näitä aihepiirejä on käsitelty tutkimalla lumen sulantapäivää sekä lumen vesiarvoa käyttäen satelliittien mikroaaltoradiometrien mittauksia.

Olemassa olevia algoritmeja on parannettu sekä on kehitetty uusia menetelmiä. Erityisenä painopistealueena on ollut boreaalinen metsävyöhyke. Työn tuloksena on saatu pitkä aikasarja lumen sulantapäivästä sekä lumen vesiarvosta. Aikasarjat kattavat yli kolmen vuosikymmenen aikajakson. Aikasarjat ovat merkittäviä ilmastotutkimuksen kannalta, esimerkiksi geofysikaalisten prosessien mallintamiseksi. Lumen sulantapäivän aikasarjaa voidaan käyttää hiilidioksiditasapainon arvioimiseksi biosfäärin ja ilmakehän välillä ja väitöksessä esitetään tästä tuloksia.

Lisäksi työssä on kehitetty menetelmiä arvioida lumen massaa pohjautuen lumen vesiarvoon pohjoisella pallonpuoliskolla ja paikallisemmassa mittakaavassa. Aikasarjojen lisäksi työn tuloksena on syntynyt myös satelliittiaineistojen lähes reaaliaikaisia tuotepalveluita hydrologiseen käyttöön. Lumen vesiarvotietoa voidaan hyödyntää mm. jokien virtausennusteissa, jotka ovat merkittäviä vesivoimayhtiöille ja auttavat myös tulvien torjunnassa.

Julkaisijayksikkö Ilmatieteen laitos

Julkaistu myös sarjassa Aalto University publication series DOCTORAL DISSERTATIONS 230/2018

Luokitus (UDK)	Asiasanat
snow 551.332 climatology 551.58 remote sensing 528.8	lumi, sulanta, vesiarvo

ISSN ja avainnimeke
0782-6117 FMI Contributions 151

ISBN	Kieli	Sivumäärä
978-952-336-065-5	Englanti	54

FINNISH METEOROLOGICAL INSTITUTE

Published by Finnish Meteorological Institute
(Erik Palménin aukio 1), P.O. Box 503
FIN-00101 Helsinki, Finland

Series title, number
FMI Contributions 151

December 2018

Author(s)

Takala, Matias

Title Microwave remote sensing of snow and environment

Abstract

Hemispheric snow extent and snow mass are two important parameters affecting the water cycle, carbon cycle and the radiation balance in particular at the high latitudes. In this dissertation these topics have been investigated focusing on the mapping of snow clearance day (melt-off day) and Snow Water Equivalent (SWE) by applying spaceborne microwave radiometer instruments.

New algorithms have been developed and existing ones have been further advanced. Specific attention has been paid to estimate snow in boreal forests. This work has resulted in Climate Data Records (CDRs) of snow clearance day and daily values of SWE. Data are available for the entire Northern Hemisphere covering more than three decades. The developed CDRs are relevant for climate research, for example concerning the modeling of Earth System processes. CDR on snow clearance day can be used to map the CO2 balance between the biosphere and atmosphere in the case of boreal forests, which is demonstrated in the thesis.

Further, methodologies to assess snow mass in terms of SWE for hemispherical and regional scales have been developed. The developed methodologies have also resulted in the establishment of new Near-Real-Time (NRT) satellite data services for hydrological end-use. In hydrology SWE data are used to enhance the performance of river discharge forecasts, which is highly important for hydropower industry and flood prevention activities.

Publishing unit Finnish Meteorological Institute

Published also in Aalto University publication series DOCTORAL DISSERTATIONS 230/2018

Classification (UDC)
snow 551.332
climatology 551.58
remote sensing 528.8

Keywords
snowmelt, hemisphere, estimating techniques

ISSN and series title
0782-6117 FMI Contributions 151

ISBN
978-952-336-065-5

Language
English

Pages
54

Microwave remote sensing of snow and environment

Matias Takala

A doctoral dissertation completed for the degree of Doctor of Science (Technology) to be defended, with the permission of the Aalto University School of Electrical Engineering, at a public examination held at the lecture hall TU1 of the school on 4 December 2018 at 12.

Aalto University
School of Electrical Engineering
Department of Electronics and Nanoengineering

Supervising professor
Prof. Jaan Praks

Thesis advisor
Prof. Jouni Pulliainen, Finnish Meteorological Institute, Finland

Preliminary examiners
PhD Jiancheng Shi, Chinese Academy of Sciences (CAS), China
Prof. Richard Kelly, University of Waterloo, Canada

Opponent
Prof. Claude Duguay, University of Waterloo, Canada

Preface

This work has been carried out first at Helsinki University of Technology in laboratory of Space Technology (which is now part of the Department of Electronics and Nanoengineering at Aalto University) and then at the Finnish Meteorological Institute. I express my gratitude to Professor Martti Hallikainen for guiding me to the field of Space Technology.

I thank wholeheartedly Professor Jouni Pulliainen for not only of a major scientific influence but also of the possibility to see from a pivotal point of view the growth of the Finnish space industry. Professor Tuija Pulkkinen gave me the necessary push and insight to finalize this thesis and professor Jaan Praks took care that the dissertation meets all the strict scientific standards. I would also like to thank all Space lab and FMI personnel for both contribution and support.

Finally, I thank my mother and father for encouragement and believing in me. I also thank Marjis for being there even though “The night is dark and full of terrors”.

Helsinki May 7, 2018 Matias Takala

Contents

List of Abbreviations

AMSR-E Advanced **M**icrowave **S**canning **R**adiometer-**E**OS

AMSR2 Advanced **M**icrowave **S**canning **R**adiometer 2

ANN Artificial **N**eural **N**etwork

API Application **P**rogramming **I**nterface

AVHRR Advanced **V**ery **H**igh **R**esolution **R**adiometer

CDR Climate **D**ata **R**ecord

DAV Diurnal **A**mplitude **V**ariations

DMSP Defense **M**eteorological **S**atellite **P**rogram

DUE Data **U**ser **E**lement

ECMWF European **C**entre for **M**edium-Range **W**eather **F**orecasts

EO Earth **O**bservation

EOS Earth **O**bservation **S**ystem

EREP Earth **R**esources **E**xperiment **P**ackage

ESA European **S**pace **A**gency

ESMR Electrically **S**canning **M**icrowave **R**adiometer

EUMETSAT European Organization for the Exploitation of **Met**eorological **Sat**ellites

FMI Finnish **M**eteorological **I**nstitute

FSC Fractional **S**now **C**over

GCW Global **C**ryosphere **W**atch

GPP Gross **P**rimary **P**roduction

HOPS Hydrological **O**perations and **P**rediction **S**ystem

H SAF Hydrology **S**atellite **A**pplication **F**acility

IMS Interactive **M**ultisensor **S**now and Ice Mapping System

MWRI Micro-**W**ave **R**adiation **I**mager

NEP Net **E**cosystem **P**roduction

NWP Numerical **W**eather **P**rediction

NRT Near **R**eal **T**ime

OGC Open **G**eospatial **C**onsortium

SAR Synthetic **A**perture **R**adar

SCD Snow **C**learance **D**ay

SE Snow **E**xtent

SD Snow **D**epth

SnowPEx Satellite **Snow P**roduct Intercomparison and Evaluation **Ex**ercise

SR Super **Re**solution or **S**pring **R**ecovery

SWE Snow **W**ater **E**quivalent

SSM/I Special **S**ensor **M**icrowave/**I**mager

SSMIS Special **S**ensor **M**icrowave **I**mager/**S**ounder

SMMR Scanning **M**ultichannel **M**icrowave **R**adiometer

WMO World **M**eteorological **O**rganization

WMS Web **M**ap **S**ervice

XPGR Cross-**P**olarized **G**radient **R**atio

List of Symbols

B Brightness

B_B Brightness of Black Body

c Speed of Light

D Difference

e Emissivity

f Frequency

h Planck constant or horizontal linear polarization

J Source Function

k Boltzmann constant

r Radius

t Time

T Temperature

T_B Brightness Temperature

v Vertical Linear Polarization

κ_e Attenuation Coefficient

λ Wavelength

τ Optical Depth

List of Publications

P1. Takala M., Pulliainen J., Huttunen M., Hallikainen M. (2008). Detecting the onset of snow-melt using SSM/I data and the self-organizing map, *International Journal of Remote Sensing*, 29(3-4), pp. 755-766, doi: 10.1080/01431160601105934.

P2. Takala M., Pulliainen J., Metsämäki S., Koskinen J. (2009). Detection of Snowmelt Using Spaceborne Microwave Radiometer Data in Eurasia From 1979 to 2007, *IEEE Transactions on Geoscience and Remote Sensing*, Vol. 47, pp. 2996 – 3007, doi: 10.1109/TGRS.2009.2018442.

P3. Takala M., Luojus K., Pulliainen J., Derksen C., Lemmetyinen J., Kärnä J.-P., Koskinen J., Bojkov B. (2011). Estimating northern hemisphere snow water equivalent for climate research through assimilation of space-borne radiometer data and ground-based measurements, *Remote Sensing of Environment* , Vol. 115, Issue 12, 15 December 2011, Pp. 3517-3529, doi:10.1016/j.rse.2011.08.014

P.4. Takala M., Ikonen J., Luojus K., Lemmetyinen J., Metsämäki S., Cohen J., Arslan A., Pulliainen J.(2017). New Snow Water Equivalent Processing System With Improved Resolution Over Europe and its Applications in Hydrology.. *IEEE Journal of Selected Topics in Applied Earth Observations and Remote Sensing* , Vol. 10, no.2, pp.428-436, doi: 10.1109/JSTARS.2016.2586179

P.5. Tedesco, M., Pulliainen, J., Takala M., Pampaloni, P. (2004). Artificial neural network-based techniques for the retrieval of SWE and snow depth from SSM/I data. *Remote Sensing of Environment*, 90(1):76–85. doi: 10.1016/j.rse.2003.12.002

P.6. Räisänen P., Luomaranta A., Järvinen H., Takala M., Jylhä K., Bulygina ON, Luojus K., Riihelä A., Laaksonen A., Koskinen J., Pulliainen J. (2014). Evaluation of North Eurasian snow-off dates in the ECHAM5.4 atmospheric general circulation model. *Geoscientific Model Development*, 7, 3037-3057, doi:10.5194/gmd-7-3037-2014.

P.7. Pulliainen J., Aurela M., Laurila T., Aalto T., Takala M., Salminen M., Kulmala M., Barr A., Heimann M., Lindroth A., Laaksonen A., Derksen C., Mäkelä A., Markkanen T., Lemmetyinen J., Susiluoto J., Dengel S., Mammarella I. Tuovinen J.-P. (2017). Early snowmelt significantly enhances boreal springtime carbon uptake. Early edition in *Proceedings of the National Acad-*

emy of Sciences of the United States of America
doi:10.1073/pnas.1707889114.

Author's Contribution

Publication 1: Detecting the onset of snow-melt using SSM/I data and a self-organizing map.

The author was the main developer of algorithms in **P.1** and created the result dataset. Author also contributed to the analysis of the results with co-authors.

Publication 2: Detection of Snowmelt Using Spaceborne Microwave Radiometer Data in Eurasia from 1979 to 2007.

In **P.2** the author continued with the algorithm development as the main contributor and was responsible for generating the result dataset that is a CDR of snow clearance dates. Author also contributed to the analysis of the results.

Publication 3: Estimating northern hemisphere snow water equivalent for climate research through assimilation of space-borne radiometer data and ground-based measurements.

In **P.3** the author contributed to the algorithm development together with co-authors and also participated in the data set generation. Results from **P.2** were used to detect snow melt. Author also contributed to the analysis of the results.

Publication 4: New Snow Water Equivalent Processing System With Improved Resolution Over Europe and its Applications in Hydrology.

In **P.4** the author again contributed to the algorithm development and contributed to the analysis of the results with co-authors.

Publication 5: Artificial neural network-based techniques for the retrieval of SWE and snow depth from SSM/I data.

The author provided preprocessed input and validation data set in **P.5**.

Publication 6: Evaluation of North Eurasian snow-off dates in the ECHAM5.4 atmospheric general circulation model.

In **P.6** the author provided CDR of snow clearance dates and commented on the analysis of ECHAM 5 results.

Publication 7: Early snowmelt significantly enhances boreal springtime carbon uptake.

The author provided satellite derived snow melt date data (**P.2**) and also was involved in the analysis. In addition, the author provided assistance in preparing images for the publication.

1. Introduction

Knowing the accurate status of the Earth's cryosphere and in particular of snow is important for climate research (Betts and Ball 1997, Déry and Brown 2007, Flanner et al. 2011, Riihelä 2013, Tao et al. 2014, **P. 2, P.3, P.6, P.7**), numerical weather prediction (Brasnett 1998, Pullen et al. 2011, de Rosnay et al. 2014), hydrology (**P.4**) and other applications. The required data can be gathered by various means (Kuusisto 1984, Kitaev et al. 2002) but remote sensing methods do provide a better temporal and spatial coverage. Spaceborne microwave radiometers (Ulaby et al. 1981) are known to be well suited for the estimation of snow cover (Tiuri et al. 1984, Chang et al. 1987, Hallikainen and Jolma 1992, Choudhury et al. 1995, Pulliainen et al. 1999, Pulliainen 2006, Saberi et al. 2017). Even though this fact has been evident for decades the lack of robust Climate Data Records (CDR) and Near Real Time (NRT) services of snow parameters has been a problem.

In this dissertation this particular research problem has been answered by developing new and enhancing existing algorithms to reliably estimate Snow Clearance Date (SCD) (**P. 1, P. 2**) and Snow Water Equivalent (SWE) (**P.3, P.4, P.5**) on hemispherical (or regional) scale.

The results of the research are the CDR's of SCD (**P. 2**) and SWE (**P.3,** GlobSnow 2018 [ONLINE]). In addition, SWE is available as a NRT service (**P.3, P.4** GlobSnow 2018 [ONLINE], SR-SWE 2018 [ONLINE], H SAF 2018 [ONLINE]). In addition, the impact of the results for climate research is demonstrated in **P.6** and **P.7**. The importance of **P.7** originates from the fact that the obtained snow parameters can be used to estimate higher lever physical parameters such as CO_2 balance (Aurela et al. 2004, Groendahl et al. 2007, Winchell et al. 2016). The application of SWE for hydrology is demonstrated in **P. 4**.

The basis for spaceborne microwave radiometry was laid in the 70's. The Nimbus 5 was launched in 1972. It had the ESMR instrument (Wilheit 1972) on board which only measured at 19 GHz by using horizontal polarization. In addition, radiometer instruments were on board Skylab space station (Eason 1978). They were part of the Earth Resources Experiment Package (EREP) experiment and were not thus operational instruments. There were two radiometry capable devices in the EREP: S193 and S194. The S193 was a micro-

wave radiometer, scatterometer and altimeter. It operated only on the frequency of 13.9 GHz. The S194 was a pure L-band radiometer operating on the frequency of 1.4 GHz and was thus best suited for the monitoring of soil moisture (Eagleman and Lin 1976). These experiments, in particular the ESMR, proved the general potential of spaceborne microwave radiometry. A significant technological advancement in the field was the SMMR (Scanning Multichannel Microwave Radiometer) instrument on board Nimbus-7 satellite (Gloersen and Hardis 1978). It was launched in October 1978 and was the first satellite to provide spaceborne radiometer data in an operative manner. Even though it only provided data every other day it still forms a crucial basis for this dissertation. The spatial resolution of these early and succeeding radiometers has been rather coarse but, on the other hand, if the satellite is on a polar orbit it can map almost the whole Earth (especially in the northern latitudes) in 24 h. As a passive method radiometry does not depend on external illumination like sunlight and it is rather insensitive to weather phenomena. Also, the potential for remote sensing of snow was acknowledged even though the frequencies used on these experiments were not optimal for this purpose.

SMMR was the first fully operational spaceborne radiometer instrument. As the name suggests it had multiple channels or frequencies it measured. The most important frequencies for remote sensing of snow were 18 GHz and 37 GHz. These frequencies made it possible to develop many remote sensing applications and boosted research significantly. This development raised interest in snow as a parameter (for example Tiuri et al. 1984). First global estimates of Snow Water Equivalent (SWE)[1] were also provided during the lifetime of Nimbus-7 and SMMR (Chang et al. 1987). SMMR was functional and provided data for eight years and ended operations in August 1987.

Fortunately, the success of SMMR was continued by new instruments. The US DMSP (Defense Meteorological Satellite Program) consists of multiple satellites for weather monitoring. Since July 1987, the SSM/I radiometric instrument has been producing data, first onboard the F-08 satellite (Armstrong et al. 1994). The SSM/I instrument has almost the same frequencies as SMMR and it provided crucial continuity in the availability of radiometer data. The SSM/I was on board satellites F-08, F-10, F-11, F-13, F-14 and F-15. Apparently SSM/I is still functional on F-15 but its data is unreliable at the moment. The evolution of SSM/I is an instrument called SSMIS (Armstrong et al. 1994), which has additional frequencies compared to SSM/I. The SSMIS instrument has been flown on board DSMP satellites F-16, F-17, F-18 and F-19. SSMIS data is available today even in Near Real Time (NRT). The SSMIS is an evolution version of SSM/I with additional frequencies for monitoring the atmosphere. The frequencies used for snow detection are the same as for SSM/I. Both SSMIS and SSM/I provide data every day, compared to SMMR.

[1] Snow Water Equivalent can be thought as the depth of the resulting water layer if snow could be melted instantaneously. SWE is snow density times snow depth so the parameter describes both mass of snow and depth.

There are also other spaceborne radiometer systems that were previously or are currently active. The NASA Aqua satellite carries the AMSR-E instrument (Kawanishi et al. 2003). It is in many ways comparable to SSM/I. Aqua satellite was launched in May 2002. While the spacecraft is still in operation, the AMSR-E instrument stopped working in October 2011. The successor of AMSR-E is AMSR2 (Imaoka et al. 2010), which is on board GCOM-W. The AMSR2 can be used for snow monitoring similar to SSMIS instruments, but from the time series continuity point of view SMMR-SSM/I-SSMIS is better suited for creating Climate Data Records (CDR). The Chinese Fengyung-3 series satellites have the MWRI instrument on board (Yang et al. 2011), which also has a suitable frequency range to estimate snow parameters. The ESA SMOS mission (Kerr et al. 2010) has an L-band radiometer, but because of the measuring frequency, its usefulness for snow detection is very limited. However, it provides information on soil frost, which is an important cryospheric application (Rautiainen et al. 2016).

Snow is an important physical parameter in terms of many geophysical processes. The albedo of snow affects directly the radiation budget of the Earth's atmosphere and thus it directly contributes to the global warming (Betts and Ball 1997, Déry and Brown 2007, Flanner et al. 2011, Riihelä 2013, Tao et al. 2014). The amount of snow in terms of both Snow Extent (SE) (or Fractional Snow Cover FSC) and snow mass (SWE) is an important indicator of climate change. Snow parameters affect also numerical weather prediction (NWP) (Brasnett 1998, Pullen et al. 2011, de Rosnay et al. 2014). Winter time snow accumulation and spring time snow melt contribute to the water cycle in the atmosphere and water bodies. Forecasting river discharges is a typical concrete problem that snow parameters can contribute in hydrology (**P. 4**). It has been also shown (Aurela et al. 2004, Groendahl et al. 2007, Winchell et al. 2016) that the snow clearance date is related to the release of greenhouse gases such as CO_2.

In situ-measurements of snow are an accurate method to provide data of SE and SWE (Kuusisto 1984). In Finland, for example, one can find a dense network of SWE measurements. However, in the Finnish case the distributed SWE observations along snow courses are only carried out once a month. Typically, such kind of national observation networks do not exist and the availability of such data from other networks (such as those maintained by hydropower companies) are limited. Pointwise synoptic Snow Depth (SD) observations from the global WMO coordinated weather station network are available daily. If the pointwise measurement locations have a dense coverage of the area it is possible to interpolate the values to a larger region with reasonable accuracy. In the arctic region there are, however, very large areas without any *in situ* data measurements whatsoever.

To provide reliable and continuous estimates of SE and SWE Earth Observation (EO) methods and remote sensing are typically a necessity. Optical in-

struments can give reliable high resolution information on SE or FSC but they are dependent on the availability of solar illumination, which is a problem at the high latitudes during the mid-winter time (Frei et al. 2012, Metsämäki et al. 2012, Metsämäki et al. 2015). During spring-winter conditions optical sensors provide proper information on global snow melt, even though some gaps exist in data products due to obscuring cloud cover (Frei et al. 2012, Metsämäki et al. 2015). However, a problem in optical satellite sensor derived CDRs is the limited availability of historical sensors and the cross calibration of differert sensors concerning the construction of long time-series of SE information (Zhou et al. 2013, Estilow et al. 2015).

In practice, it is not possible to estimate SWE with optical instruments. Thus, microwave region is better suited for snow monitoring (Pulliainen et al. 1999, Foster et al. 2005, Frei et al. 2012). Synthetic aperture radar (SAR) can be used to a degree to estimate SWE (Macelloni et al. 2014). However, there are problems with the reliability of SWE detection and even though the spatial resolution of radar image is high getting coverage over a large area within 24h is not easy. Microwave radiometers offer good detection of SWE (and SE) with full coverage over continental and hemispherical scale and for long time periods (**P.2**, **P.3,** Pulliainen 2006). Estimating SWE from microwave data has its problems too. Complex topography, vegetation cover, water bodies and wet snow have an effect on the SWE retrieval.

Snow melt or snow clearance day algorithms using microwave radiometer data have mostly been applied over ice or glaciers and not over arctic tundra or taiga (Abdalati et al. 1995, Drobot et al. 2001, Smith et al. 1998, Hall et al. 2004). In this dissertation algorithms were specifically developed and tested for forested areas. The result is a CDR of snow clearance day covering the Northern Hemisphere and spanning over 30 years (**P. 2**). The CDR is also validated using independent ground reference data. The best approach of SWE retrieval has turned out to be a data fusion of synoptic SD observations and spaceborne SWE estimates (Pulliainen 2006, **P.3**). In this dissertation the SWE algorithm introduced by Pulliainen (2006) has been further developed to be feasible for operational use and to construct a CDR of SWE covering the Northern Hemisphere for over 30 years (**P. 3**). The SWE CDR is validated with independent ground reference data obtained for snow courses from northern Eurasia. In addition, the SWE algorithm has been improved to yield a higher spatial resolution over Europe by applying a superresolution inversion approach (**P. 4**).

The resulting data sets have been applied in addressing several research questions The CDR of SCD has been used as a reference to ECHAM5 global circulation model predictions to assess the performance of the model in snow covered regions (**P. 6**). The results show that the ECHAM5 model snow predictions are in line with the satellite based SCD dataset. The snow melts first in the Baltic regions in March and last in Taymyr Peninsula (in June) and the northeastern parts of Russian Far East. There is a delayed snow melt in southeastern Siberia

and an early bias in the western and northern parts of northern Eurasia. In **P.7** the CDR is used as a proxy indicator to estimate the change of gross primary production (GPP) of CO_2. The results indicate that the CO_2 uptake has increased in Jan-June by 8.4 gCm^{-2} (3.7%) per decade. The CDR is also a basic data set applicable to various other research purposes.

The SWE CDR (**P. 3**) has been created as part of ESA DUE GlobSnow project that aimed to the provision of scientific basic data set for climate research purposes (CDR on global snow cover). In addition, the work has resulted in the development and enhancement of operational snow monitoring services in EUMETSAT Satellite Application Facility for Hydrology (H SAF) (**P. 4**). The obtained SWE estimates have also been tested to be used as an input to hydrological modeling indicating that the derived satellite data-derived SWE information can be used to improve river discharge forecasts (**P. 4**). Thus, the main focus of this thesis has been in the creation of CDR's of SWE and SCD. The secondary focus has been applying the algorithms in operational services. In addition, the use of the results in the context of climatology and hydrology has been demonstrated.

2. Review of algorithms to estimate Snow Clearance Day and Snow Water Equivalent from brightness temperature signatures

Passive microwave radiometry is the most feasible remote sensing method to map snow parameters in hemispherical scale since most of the area can be covered within 24 hours. Essentially, all matter emits thermal radiation, which can be used to deduce physical properties of the source. There are several snow remote sensing products available but there are issues with, for example, temporal and spatial coverage and complete or partial lack of validation. The work conducted in this dissertation addresses many of these issues. Long time series are based on SMMR, SSM/I or SSMI/S instrument data on board Nimbus-7 and various DMSP-series satellites.

2.1 Brightness temperature and radiative transfer theory

All matter emits thermal radiation. Brightness of a black body is determined by Planck's Law (Ulaby et al. 1981):

$$B = \frac{2hf^3}{c^2}\frac{1}{e^{\frac{hf}{kT}}-1}, \qquad (2.1\text{-}1)$$

where B is brightness, h is Planck constant, f is frequency, c is speed of light, T is temperature and k is Boltzmann constant.

In case of microwaves $hf<<KT$ and equation can be simplified to (Ulaby et al. 1981):

$$B = \frac{2kT}{\lambda^2}, \qquad (2.1\text{-}2)$$

where λ is the wavelength. This is called Rayleigh-Jeans law. Natural bodies are not black bodies but rather grey bodies. Then one can define emissivity (Ulaby et al. 1981):

$$e = \frac{B_B}{B} = \frac{T_B}{T}, \quad (2.1\text{-}3)$$

where B_B is the brightness of grey body and B brightness of black body, correspondingly T_B is the brightness temperature and T is temperature.

Emissivity on the other hand depends on viewing angle and permittivity of the medium, which further depends on frequency and other physical parameters. The only parameter measured by airborne or spaceborne radiometers is the intensity of the radiation. Because of the linearity of the Rayleigh-Jeans Law this is usually expressed as brightness temperature.

Due to the athmosphere the brightness of the source is affected by the scattering and absorption. To deduce the true brightness of the source, one must use the radiative transfer equation (Ulaby et al. 1981):

$$B(r) = B(0)e^{-\tau(0,r)} + \int_0^r \kappa_e(r')J(r')e^{-\tau(r',r)}dr', \quad (2.1\text{-}4)$$

where B is brightness, r is radius, τ optical depth, κ_e attenuation coefficient and J source function. The interpretation of the transfer equation is that at the distance r from the source the first term describes brightness in the source (r=0) that is attenuated exponentially. The second term contains losses and gains by absorption, scattering and emission in the path of radiation from source to distance r. In practice, this means contributions from vegetation and atmosphere when snow covered terrain is considered as the target of remote sensing observations.

In the case of snow previous research has shown that the most important frequencies of satellite observations are 18 GHz and 37 GHz concerning the estimation of SWE (Chang et al. 1987, Choudhury et al. 1995, Saberi et al. 2017). Since the volume scattering inside a snow pack due to snow grains increases with frequency, the difference in brightness temperature between these frequencies increases with increasing snow mass (SWE), given that the snow grain size is constant (Chang et al. 1987). Hallikainen and Jolma (1992) have shown that the best correlation with increasing SWE can be obtained by using a channel difference of 18 GHz and 37 GHz vertical polarization in the case of satellite observations.

2.2 Review of algorithms to estimate snow melt

Frequencies in the ranges of 18 to 19 and 36 to 37 GHz and their channel differences or so called cross-polarized gradient ratios form the basis of detecting snow melt in microwave domain. Abdalati et al. (1995) and Hall et al. (2004) used cross-polarized ratio:

$$\mathrm{XGPR} = (T_{19h} - T_{37v})/(T_{19h} + T_{37v}), \quad (2.2\text{-}1)$$

where v and h refer to vertical and horizontal polarizations and 19 and 37 to the frequencies of the received signals.

On the other hand, Smith (1998) used only a channel difference of these frequencies with horizontal polarization to map primarily the onset of sea ice melt. According to Smith, the rapid change of brightness temperatures is first related with the increase of the moisture in the snow pack on top of the ice layer. Thus the algorithm is, at least partially, applicable to the detection of snow melt. Drobot and Anderson (2001) applied a similar approach with vertical polarization.

Neural network algorithms (ANN) have not been widely applied to estimate the onset of snow melt. In **P. 5** ANN's were used to estimate SWE and SD. Simpson et al. 2001 used ANN with AVHRR data. Neural networks were also tested in **P. 1** to retrieve snow melt information.

Joshi et al. (2001) used channel differences over Greenland together with time series analysis to estimate the snow melt. The problem is that their work is based on the detection of snow over ice and thus it is not directly applicable to boreal forest zone. Mognard et al. (2003) used channel difference of horizontal polarization to calculate the time series of snow melt globally and their dataset covers 20 years. However, the dataset is not validated at all.

Ramage and Isacks (2002) utilized the Diurnal Amplitude Variations (DAV) of 37 GHz vertical polarization channel to estimate snow melt over glaciers in Alaska, USA and British Columbia, Canada. DAV is the difference between the brightness temperature signatures of usually early morning and late afternoon. This approach is convenient because it allows the retrieval of temporary snow melt occurences too. The main emphasis on the work in this thesis, however, has been estimating the snow clearance date only.

The main shortcoming of earlier work is the lack of comprehensive validation. The scarcity of ground reference data is the first and foremost problem. In order to provide a reliable CDR, validation of the algorithm is a necessity. It is especially important, if one wishes to do hemispherical scale mapping (Mognard et al. 2003) for longer time periods spanning over decades (Abdalati et al. 1995, Hall et al. 2002 and 2004). Foster et al. (2005) have used weather observation and in situ radiometer data to validate satellite estimates in tundra, but their work does not cover recent times.

Most of the work carried out earlier (Abdalati et al. 1995, Hall et al. 2002, Drobot et al. 2001, Smith et al. 1998, Ramage and Isacks 2002) is applicable only over glaciers and thus cannot be used to estimate snow melt in hemispherical scale.

The biggest challenge for snow melt estimation is the forested regions on Earth such as the Taiga belt. Either the algorithms do not work well over forest or the coverage is limited. Results of Smith et al. (1998) and Mognard et al. (2003) do include forested regions but, as mentioned before, have either methodological shortcomings or lack comprehensive validation.

One should also notice that many of the snow melt algorithms described detect the onset of snow melt instead of the snow clearance date, which has been the main focus in this dissertation. The snow clearance date has been more relevant for the detection of greenhouse gasses (**P.7**). However, the algorithms developed in this dissertation (**P. 2**) can be modified to detect the onset of snow melt as well.

2.3 Review of Snow Water Equivalent algorithms

As mentioned earlier in 2.1, the most important frequencies for snow detection are 18 and 37 GHz. Chang et al. (1987) proposed an algorithm where Snow Depth (or SWE) is directly proportional to the channel difference of 18 GHz and 37 GHz channels (horizontal polarization) based on simulation experiments with a radiative transfer model. This is a simple and robust algorithm for SWE retrieval. Even if the approach by Chang et al. (1987) and its developments (Choudhury et al. 1995, Kelly et al. 2003, Tedesco et al. 2010, Saberi et al. 2017) may perform well regionally, there are major problems in applying the approach to hemispheric scale. Validation of the SWE estimates with available *in situ* data has demonstrated this, see **P.3**. This simple algorithm does not take into account special cases such as wet snow, regional variation such as vegetation and land use or grain size of snow. The approach by Chang et al. (1987) has been further enhanced by taking into account the forest cover fraction (Foster et al. 2005). The current baseline of NASA SWE algorithm (Kelly et al. 2003, Tedesco et al. 2010) has a better handling of forested areas and it takes wet snow areas into account. All SWE algorithms have a tendency to underestimate SWE under deep snow conditions and when snow is wet. However, the effect is more pronounced with channel difference type of algorithms.

Artificial neural networks are one possibility to try to map SWE from brightness temperature (**P. 5**). Chang and Tsang (1992) used a neural network trained with a dense media multiple scattering model together with inversion to estimate SWE. The input data consisted of SSM/I brightness temperatures from the channels 19, 22 and 37 GHz. Their results gave SWE retrieval error ranging from 9% up to 57%. However, neural networks have not been widely applied to estimate SWE.

Instead of using empirical approach, theoretical or semi-empirical radiative transfer models can be used for snow cover detection. They typically include the effect of atmosphere and vegetation. Microwave emission can be estimated using the model and thus obtain estimates of SWE through inversion (Pulli-

ainen et al. 1999, Pulliainen 2006, Wiesmann and Matzler, 1999). Models are typically computationally expensive and also require additional input and auxiliary data to get estimates of SWE, accurate enough e.g. for the hydrological end-use (Durand et al. 2008). This restricts their use both on regional and hemispherical scale.

One option to improve passive microwave retrieval algorithms is to use data assimilation. This has been investigated by Pulliainen (2006), where an assimilation technique is presented using passive microwave data combined with a semi-empirical radiative transfer model together with *a priori* snow data from ground measurements with corresponding statistical uncertainties. When snowpack gets thicker there are systematic errors caused by the saturation of the observed brightness temperature (T_B), which also affects the channel difference algorithms. The saturation is caused by the fact that after a certain threshold of snow depth the brightness temperature signal from the ground is attenuated and T_B ground reference level changes. Data assimilation reduces these errors when SWE exceeds about 120 mm. Concerning SWE estimation error characteristics unbiased Root Mean Squared Error (RMSE) values between 15 to 40 mm can be achieved by comparing with *in situ* data (Pulliainen and Hallikainen 2001, Pulliainen 2006).

The simplest way to estimate SWE is to interpolate local SWE observations for a larger area and thus get an estimate of the hemispherical or regional SWE. On the other hand, if the local observation network is sparse then in large areas the estimates are based on SD values maybe tens or even hundreds of kilometers away. In practice, interpolation as a sole method is possible only in few regions, where the network is dense. In remote areas, the only realistic estimate can be obtained by using spaceborne SWE estimates.

3. Advances in snow monitoring - results and discussion

This thesis focuses on advances in snow monitoring obtained by using space-borne passive microwave remote sensing, that is space-borne microwave radiometry. The developed and applied methods are tested and validated in regions representing boreal forests, tundra and steppe, thus making the methods valid for major parts of the northern hemisphere. In addition, the algorithms have been used to generate CDRs spanning over three decades. The developed algorithms are applicable to operational services both in hemispherical and regional scale, which is also demonstrated.

3.1 Materials

The radiometer data used in this work consists of brightness temperatures measured by SMMR (Knowles et al. 2002) on board Nimbus-7 and SSM/I and SSMIS data (Armstrong et al. 1994) on board various DMSP-series satellites. The data covers Northern Hemisphere spanning over 30 years.

The SWE algorithm (Pulliainen et al. 1999, Pulliainen 2006, **P. 3**) uses synoptic SD data as input. These data are obtained from European Centre for Medium-Range Weather Forecasts (ECMWF). For the operational implementation (**P. 4**) the data is acquired from Finnish Meteorological Institutes (FMI) near real time database.

For the validation of SCD (**P.2**) and SWE the INTAS SCCONE (Kitaev et al. 2002) material has been used. It consists of two datasets, SWE path measurements and SD measurements with observation flags over Eurasia. The SWE path data was used in validating the spaceborne SWE estimates where as the SD measurement flags were used to to estimate the accuracy of SCD retrieval. In addition, for the validation of the SWE estimates also Finnish Environment Institutes (SYKE) SWE measurements (Kuusisto 1984) were used. Experimental datasets (Derksen 2008, Derksen et al. 2009) in Canada were used to validate SWE for North America.

The land use data in **P.3** was based on Global Land Cover 2000 (GLC 2003). Forest Cover Fraction was also calculated using GLC2000. For North America stem volume had a constant value, where as for Eurasia a variable stem volume based on Bartalev et al. 2004 was applied. The topography data was ETOPO5 (ETOPO5 1990 [ONLINE]). In **P.4** the land use was based on ESA GlobCover 2009 data (Bontemps et al. 2011). The forest stem volume map was also changed and the details are described in **P.4.** The topography data was again based on ETOPO5.

In **P.3** the snow covered area masking is based on the wet snow algorithm by Hall et al. (2002) in the autumn and on the SCD dataset (**P.2**) in the spring. In **P.4** the masking is done by using Interactive Multisensor Snow and Ice Mapping System (IMS) data (National Ice Center 2008).

3.2 Snow melt off and dry snow mapping

Snow melt by empirical channel difference algorithms

Channel difference algorithms have been widely applied in order to detect snow melt from space-borne microwave radiometer data (Smith 1998, Drobot et al. 2001). The algorithms are based on the fact that for dry snow scattering dominates causing a spectral gradient in the observed microwave signatures, whereas for wet snow the absorption or reflection from the air-wet snow boundary dominates causing a change in spectral signatures. Such an algorithm using discrete thresholds for wet snow detection is described and employed in **P. 1**:

$$(T_{37v}-T_{19v})> -21 \text{ K} \qquad (3.1\text{-}1)$$

and

$$(T_{37h}-T_{19v})< -10 \text{ K}. \qquad (3.1\text{-}2)$$

When conditions according to criteria (3.1-1) and (3.1-2) are valid for the investigated pixel, it is interpreted to represent melting snow conditions.

Dry Snow mapping by empirical channel difference algorithms

An empirical channel difference algorithm to detect dry snow cover was introduced by Hall et al. (2002). First, the algorithm determines snow depth (SD) [cm] by

$$SD=15.9(T_{19h}-T_{37h}), \qquad (3.1\text{-}3)$$

where T is brightness temperature and sub-indices denote the channels. If the conditions

SD > 80 cm and T_{37v} < 250 K and T_{37h} < 240 K (3.1-4)

are met the data is classified as dry snow. This threshold algorithm is applied to provide information on snow extent in **P.2** and **P.3**.

Self-organizing map based snow melt detection algorithm (P. 1)

Self-organizing map (SOM) (Kohonen 1982) is a neural network consisting typically of a 2D layer of neurons. A neuron is a computational unit that has a weight vector specific to the neuron and an input vector that is common for every neuron. SOM has two phases of operation, the learning phase and the running phase of a trained network.

The running phase is based on the competitive process. It means that for each neuron the Euclidean distance between input and weight vectors are determined and the neuron with the shortest distance is considered to be the winning neuron or the neuron that is activated. The activated neuron is considered to represent the class of vectors to which the input vector belongs to.

In the learning phase the neurons are first assigned with random weight vectors. The input vector is fed to the neurons and the winning neuron is determined (like in the running phase). Then the weights of the neuron are adjusted according to the SOM algorithm (Kohonen 1982). The amount of adjustment is a function of time (the amount of adjustment grows smaller in time). In addition, the adjustment is not performed only for the winning neuron but to the adjacent neurons as well. The neighbourhood function is typically Gaussian and its width shrinks also in time. Once the weights converge the learning phase is finished.

The input vector for SOM in this dissertation is $T=[T_{19v}\ T_{22v}\ T_{37v}\ T_{19h}\ T_{37h}]$. The size of the SOM 2D lattice was chosen to be 3x3 so that the classification would not be too fine grained. First the SOM was trained with a set of brightness temperatures having a large areal and temporal coverage. Once the network was settled it was fed with brightness temperatures that correspond to cases where snow depth is less than 1 cm and the winning neuron was then determined as the neuron activated most often.

Feedforward neural network based snow melt detection algorithm (P. 1)

The feedforward network (Haykin 1999) typically consists of three or more 1D layers of neurons. For the hidden layer the input is the input layer vector. The output of the hidden layer is then the input for the next layer. Like the SOM,

feedforward network has a learning and running phase. Unlike the SOM, this type of ANN learns only supervised.

The input layer consists only of the input vector, where as the hidden and output layers have computation neurons. For each hidden or output layer neuron there is a weight vector and input vector. A single neuron calculates the dot product of input and weight vectors. In addition, there can be additional terms such as bias term and an activation function for the output. In the running phase the input signal first propagates from input layer to hidden layer (or layers) and from there to the ouput layer.

The learning phase of the network is supervised, which means that for each input vector there is a corresponding desired output. The input vector is presented to the network and the resulting output is calculated. Then the difference between the obtained output and desired ouput is calculated and the relative error is backpropagated to the neurons until to the input layer. The weights are adjusted accordingly. The relative amount of the adjustement decreases in time (as with the SOM) so that the network will reach a state of equilibrium. Then the learning is finished.

In this work the network consists of only one hidden layer of 5 neurons and one output layer. The input vector $T= [T_{19v}\ T_{22v}\ T_{37v}\ T1_{9h}\ T_{37h}]$ is the same as for the case of SOM. The activation function is sigmoidal. In the training phase the desired ouput has been set to 1 if SD is less than 1 cm and 0 otherwise for each corresponding brightness temperature vectors. Like in the case of the SOM the training data set consisted of brightness temperatures having a large areal and temporal coverage. Teaching data was also separate from the actual test data presented to the network.

Snow melt detection based on time series analysis (P. 2).

The melt detection algorithm using brightness temperature observation time series is based on the detection of changes similar to the threshold algorithms discussed above. The additional feature is that the changes are not detected from a single (vector of) multi-channel observation occurring at the time of interest, but from a history of observations. The developed algorithm is based on the analysis of channel difference D (T_{37V} - T_{19v}) with the parameter t_N ranging from 1 to 180 days (where 1 is the first day of the year):

$$D(t_N) = T_{37v}(t_N) - T_{19v}(t_N), \qquad (3.1\text{-}5)$$

where $D(t_N)$ is averaged in time with a window of length 8 (N=7, N is the day under investigation) and maximum and minimum values are determined:

$$D_{max,tavg} = max\langle D(t_0), D(t_1), \dots, D(t_N)\rangle, \qquad (3.1\text{-}6)$$

$$D_{min,tavg} = min\langle D(t_0), D(t_1), \ldots, D(t_N)\rangle. \quad (3.1\text{-}7)$$

Using maximum and minimum values a threshold is determined and if condition

$$\langle D(t_N)\rangle \geq p \cdot \left[D_{max,tavg} - D_{min,tavg}\right] + D_{min,tavg}, \quad (3.1\text{-}8)$$

were the $\langle D(t_{N)}\rangle$ denotes the time average (with window length of 8 days) of $D(t_N)$ (t_N ranging from 1 to 180 days). If the condition takes place the corresponding time t_{DOY} is considered to be the time of snow melt. Of multiple occurences of t_{DOY} only the latest one is recorded. Typically, the value of p is 0.9, (**P. 2**).

Performance of snow melt detection using space-borne microwave radiometry

The comparison of different algorithms was carried out by using the INTAS SCCONE ground reference dataset indicating the time of snow melt among other snow characteristics from *in situ* observations from the Former Soviet Union (Kitaev et al. 2002). Even though the ground reference consists of pointwise measurements and the radiometer data pixel is huge (625 km²), it was shown in **P. 2** with FSC that the data are comparable. The results show that the most accurate algorithm is the one based on time series analysis. Histograms of the obtained estimation error characteristics are presented in Figure 1 for the time series algorithm. Depending on the satellite instrument the mean difference in detecting snow clearance from the landscape is 0.6-1.1 days and RMSE 22.2-22.5 days, respectively.

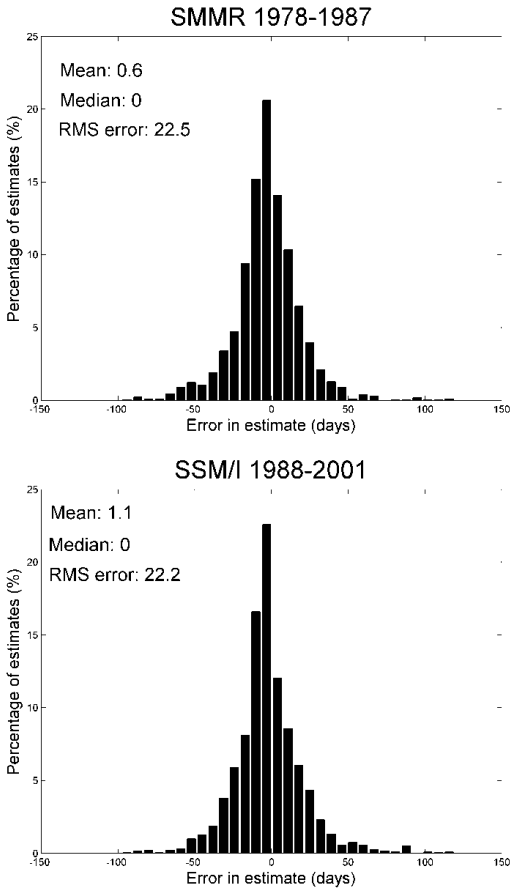

Figure 1. The accuracy of the time series snow clearance day detection algorithm (**P. 2**) copyright IEEE

The methodology using time series analysis was applied to SMMR and SSM/I radiometer observations resulting in a CDR of snow clearance day in Eurasia covering a period of over 30 years. Examples of the obtained snow clearance day estimates are illustrated in Figure. 2.

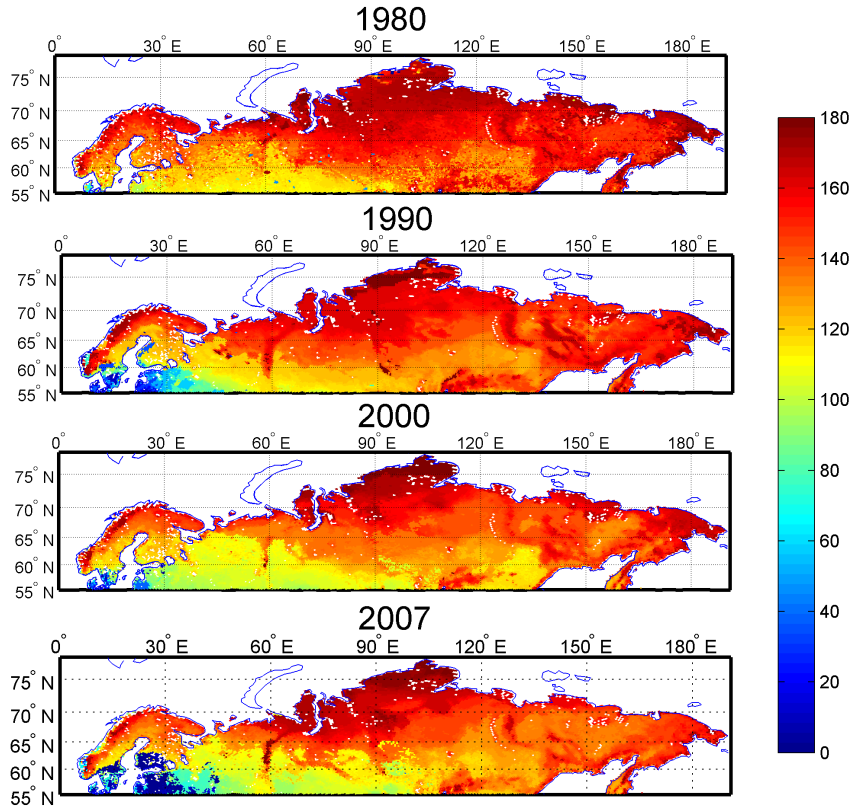

Figure 2. Snow clearance day in Eurasia for years 1980, 1990, 2000 and 2007 (days since the 31st of December of the previous year). (**P.2**) copyright IEEE

Since the snow clearance dates are known for over 30 years it is possible to estimate the trend by using linear regression. In Figure 3. the coefficient of slope is presented for ground reference data and spaceborne derived estimates. The results show that according to ground reference data the snow melts earlier in some *in situ* locations and later on in others. On the other hand the satellite interpretation mostly shows earlier show melt, excluding some mountain regions and the Taimyr peninsula.

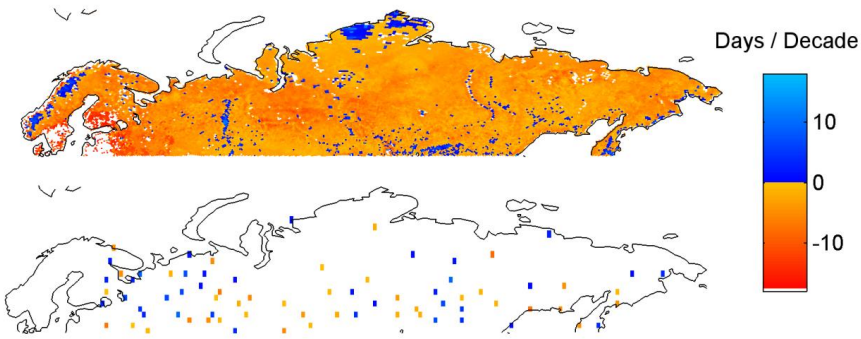

Figure 3. Trend of snow clearance date using spaceborne derived results (up) and station data (down) (**P.2**). Copyright IEEE

The time series algorithm for snow clearance day was also used in the hemispherical SWE product (see 3.2 below) as a mask to determine the snow-free areas during the spring melt period. Even though the algorithm was validated with reference data only from Eurasia, it was applied over North America too. The validity of this extension was tested as additional work for this dissertation and the results are not published before. The results are shown in Figure 4. Only areas with forest or tundra were chosen for this comparison and the land use was determined by using ESA GlobLand data, now part of Copernicus consortium (GlobLand [ONLINE]). Snow clearance date was determined from synoptic SD observations in the simplest manner. First one determines the last day when SD > 0 cm during the spring and sets the next day to be the snow clearance date.

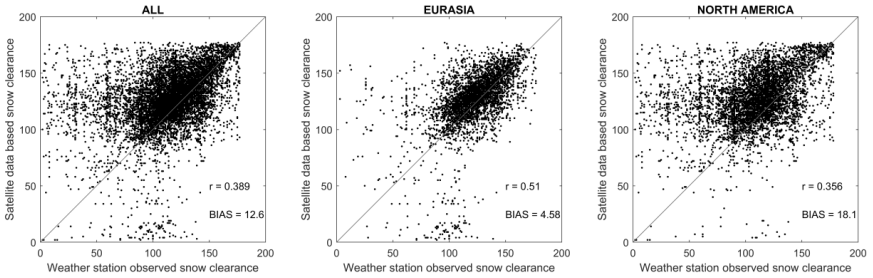

Figure 4. Direct comparison of snow clearance day estimates with weather staion observed synoptic snow depth data: (left) for whole Northern Hemisphere, (center) for Eurasia and (right) for North America. Unpublished result.

The results show that for Eurasia the estimates correspond to reference data well. In North America the algorithm works in general, but there are more cases where the ground reference shows much earlier snow melt than the satellite derived product. However, this may be explained by the fact that weather stations in North America are situated more often at airports than in Eurasia, hence representing more often open areas than forested regions.

The changes in timing of Snow Cleareance Day (SCD) have impact on both climate and ecological patterns. In particular, the SCD data set was used in **P.7**. as a proxy indicator for Spring Recovery (SR). The SR is defined as the time when CO_2 uptake exceeds 15% of the summer time maximum. The justification to use SCD as a proxy for SR is based on the fact that snow melt, soil thaw, onset of transpiration and photosynthesis take place in the same, or within a very short time frame.

P.7 managed to establish the relation between SCD and SR using CO_2 flux data from ground-based stations in Finland, Sweden, Canada and Russia (these stations measur the CO_2 flux between the ecosystem and the atmosphere using an eddy covariance method). First, a linear relation between SCD and SR was established using the flux data measured in these locations. The obtained (average) linear relation is

$$SR = 0.72 \cdot SCD + 26.22. \quad (3.1\text{-}9)$$

Once the relation is known in the measurement locations the SR can be estimated for the Northern Boreal forest zone using satellite derived SCD data. Using the resulting proxy SR estimates the trend of advanced spring recovery of carbon uptake was determined in the evergreen boreal forests. Covering the years 1979-2014 the estimated trend of advanced spring recovery turned to be 8.1 days (2.3 days per decade).

One can determine the change of Gross Primary Production (GPP) or Net Ecosystem Production (NEP) of CO_2 from the flux measurements in terms of the change of SR. Because SR is a proxy of SCD, also the change in GPP (or NEP) can be estimated using spaceborne derived data. The results show that the January-June sum of GPP has increased by 29 $g{\cdot}C{\cdot}m^{-2}$ which is 8.4 $g{\cdot}C{\cdot}m^{-2}$ (3.7%) per decade. For comparison, the obtained climate-ecosystem model predicted figures are 15.5 $g{\cdot}C{\cdot}m^{-2}$ (6.8%) per decade for Eurasia and 9.8 $g{\cdot}C{\cdot}m^{-2}$ (4.4%) for North America. Thus, the results obtained by using SCD as a proxy indicator for SR are in line with the model predicted figures.

The significance of the obtained results is also that 1) spaceborne derived estimates of physical (snow) parameters can be used as a proxy for higher level parameters. In addition, this approach 2) enables to extend the fixed location measurements both spatially and temporally. Possible shortcomings of the method appear in the areas where snow cover is ephemeral and the SCD estimates are poor. However, the number of such pixels is low compared to the overall number of pixels. Some error can be caused due to the fact that the area of one radiometer instrument pixel is 625 km^2 where as the flux measurements are conducted in a lot smaller area (few hundreds of hectares).

3.3 Snow Water Equivalent

The Snow Water Equivalent algorithm is based on assimilating ground based synoptic Snow Depth (SD) measurements with spaceborne brightness temperature observations that are modelled as a function of SWE. HUT (Helsinki University of Technology) semi-empirical algorithm (Pulliainen et al. 1999) is used to model the brightness temperatures and Bayesian likelihood method is used to invert the model to obtain a SWE estimate.

The HUT snow microwave emission model is a radiative transfer-based semi-empirical model, which estimates the emission of a homogeneous snowpack as a function of SWE, effective grain size and snow density (Pulliainen et al. 1999). The effects of soil surface, vegetation and atmosphere are considered by using empirical and semi-empirical formulas.

The SWE algorithm is based on fusing ground based Snow Depth (SD) observations from synoptic weather stations with spaceborne observations of brightness temperatures that are linked to SWE by an analytical model and with statistical error considerations. In step 1) the SD estimates are kriging interpolated over the grid. In step 2) the effective grain size and error are estimated for the SD measurement locations using the HUT model. Once the estimates are obtained the values are interpolated over the grid in step 3). Finally in step 4) the SWE estimate is obtained by using data fields from steps 1)-3) together with auxiliary data as an input. A cost function is minimized considering the observed brightness temperatures and the estimated statistics of the parameters.

The kriging interpolated SD field from step 1) forms the basis of the SWE estimate. The main sources of error in this step originate from the inaccuracies of the synoptic SD measurements. Occasionally some stations e.g. report too high values of SD and if the station location is somewhere where the network of stations is sparse the reported value can have an effect on a very large area. (**P.3**). A second source of error is the constant snow density of 0.24 g/cm^3. This is a good average value (Sturm et al. 2010) but in reality the snow density varies. Thus, SD observations may shift SWE estimates towards underestimates, if the snow density is in reality higher than 0.24 g/cm^3, or vice versa.

In step 4) the snow grain size is treated as an optimization parameter constrained by the statistics derived from steps 2-3). I case of sparse synoptic station network, this approach causes a decrease in accuracy when the distance to station increases. However, the obtained spatially and temporally varying snow grain size estimate reduces the problems caused by the strong sensitivity of space-borne observed brightness temperature to snow grain size. In the assimilation step 4) the error of kriging interpolation is also used to estimate the sensitivity of the brightness temperature to SWE. This is used as a criteria to determine how much weight is put on the ground based and spaceborne derived SWE field, which also improves the performance of SWE retrieval. In P.3 it is shown that the accuracy of SWE retrieval is improved in 60% of the cases when assimilated SWE is compared to the SD interpolated field only, Pulliainen (2006).

The effect of auxiliary parameters such as vegetation is minor compared to the main factors affecting the accuracy of the algorithm. In **P. 4** the forest stem volume map was improved compared to the map in **P.3** but without a significant effect on the SWE retrieval error. However, non published results show that the improved vegetation data might improve the retrieval error especially in the case of thick snowpack.

In Figure 5. an example of the SWE algorithm (**P. 3**) is presented. One can see how the SWE situation evolves in spring 2003. The snow extent is already almost maximum during January and in February the biggest changes are in the

snow mass given by SWE. In March the amount of snow has grown especially in Northern America. In April one can see the effect of spring time snow melt, especially in the extent of snow.

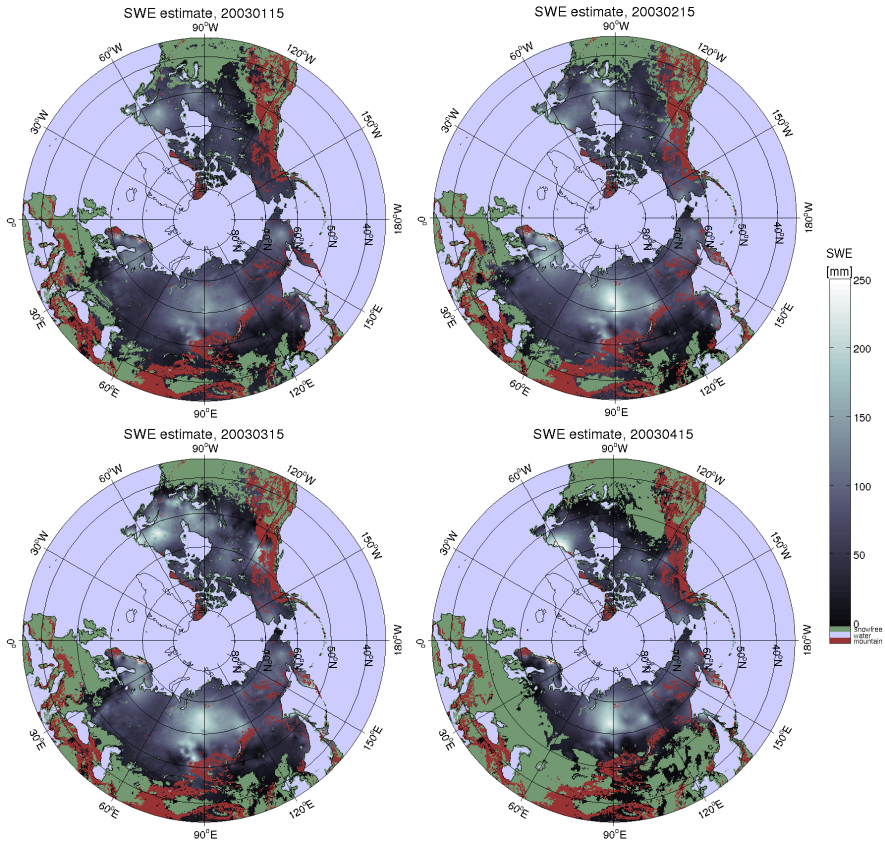

Figure 5. Example of Snow Water Equivalent (SWE) development over Northern hemisphere on 2003 (**P.3**).

The SWE results are validated against ground reference data consisting of INTASS SCCONE snow course SWE measurements in Russia covering 1979-2001, Figure 6. On the x-axis is the ground reference SWE, and the GlobSnow SWE estimate is on the y-axis. The image is divided into 5 mm x 5 mm cells and the value of each cell shows the number of value pairs falling into that category.

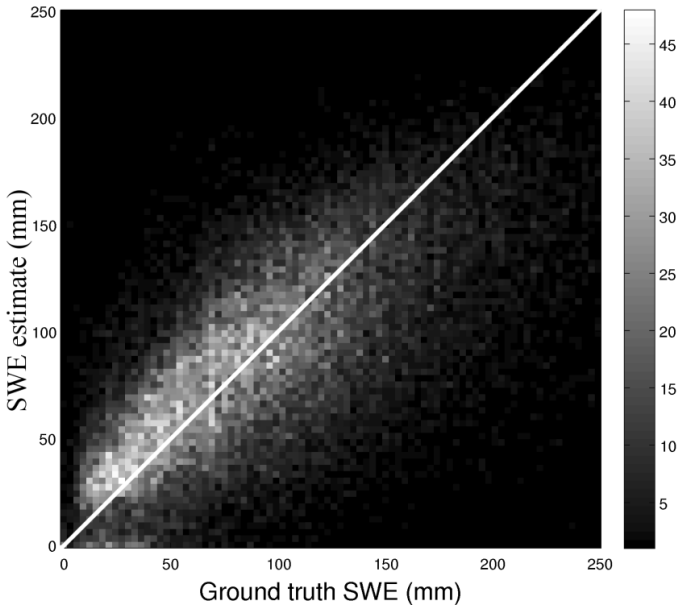

Figure 6. Density-scatterplot of ground reference SWE vs. GlobSNow SWE estimate (**P.3**).

Figure 6. shows, that the correlation between the ground reference SWE and SWE estimate is good up till the value of 150 mm, where the estimates tend to saturate. On the other hand, one can deduct from the image that the majority of Eurasian observations are well under that limit. The ground reference data consists of snow courses that typically have a length of several kilometres. The snow courses were chosen over pointwise measurements in order to better represent the large radiometer pixel (625 km^2).

Super resolution SWE estimation approach

P.4 investigated the development of SWE estimation method for a denser spatial grid by applying super resolution techniques within the assimilation scheme. In practice, this was performed by considering land cover information required as a priori information to brightness temperature model using a convolution window (moving average). Concurrently the same convolution window was applied to represent the brightness temperature in the same (oversampled) grid with a size of about 5 km x 5 km.

In Figure 7 an example of the SR-SWE estimate for the Pan European area is presented (**P. 4**) in the same way as in Figure 5 for the coarser grid covering the entire Northern Hemisphere from the latitude of 35°. In the uppermost image SWE is shown for November 2012, in the center imagefor January 2013 and in the bottom for March 2013, respectively.

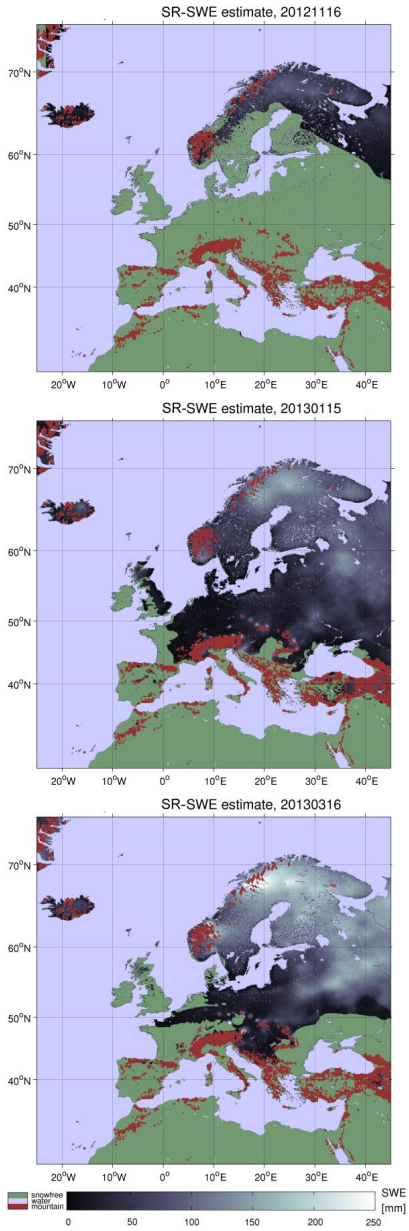

Figure 7. SWE development in Europe 2003 according to SR-SWE product (**P.5**). copyright IEEE

Figure 8. presents (**P. 4**) the comparison of the resolution of (25 km) GlobSnow SWE, GlobSnow SWE interpolated to the 5 km grid and SR-SWE 5-km-resolution. The results show that for the investigated coastal target area the radiometer native resolution of 25 km is rather coarse. The directly interpolated resolution has a better appearance, but effectively it does not show more details, whereas the SR-SWE super resolution approach has increased sub-pixel details compared to the native radiometer resolution.

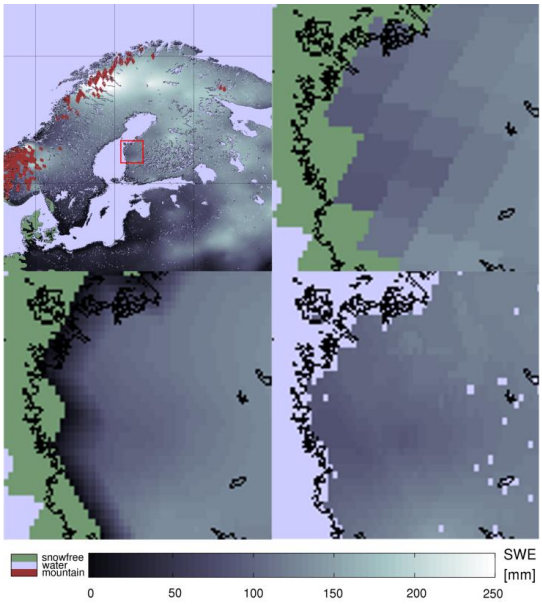

Figure 8. Example of resolution enchanment in SR-SWE product. Upper left: The area of interest. Upper right: 25 km SWE product shown in the grid of 5 km x 5 km by using the nearest neighbor interpolation. Lower left: the 25 km SWE product interpolated to 5 km grid using bilinear interpolation. Lower right: the SR-SWE product (P. 5). copyright IEEE

Experiments to assimilate Snow Water Equivalent estimates to hydrological modelling

Figure 9. presents a river discharge forecast for Ounasjoki basin using Hydrological Operations and Prediction System (HOPS) model (**P. 4**). HOPS is a hydrological model based on the Sacramento Soil Moisture Accounting Model (Burnash 1995). To take into account the potential evapotranspiration it uses a model based on Hamon's approach (Oudin et al. 2004). HOPS also contains in-house developed temperature index snow model, distributed routing model accounting for overland and channel flow retention and attenuation (**P.4**). In Figure 9. a simulation runregularized with SR-SWE product and the actual observed river discharge is shown. The results show that the regularization of the HOPS model with SR-SWE data may improve the river discharge forecasting accuracy.

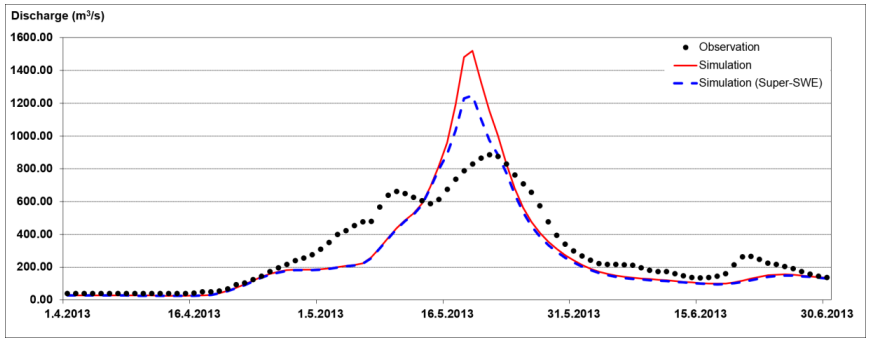

Figure 9. River discharge in Ounasjoki basin in 2013. Forecasted discharge using HOPS model, forecasted discharge with SWE data fusion and observed discharge(**P.5**). Coypright IEEE.

Monitoring of the Earth's cryosphere

The cryosphere (including snow as a parameter) is a very valuable climate change indicator yet not widely publicly acknowledged as such. The Global Cryosphere Watch (GCW) of World Meteorological Organization (WMO) is an international mechanism that supports all key cryospheric *in-situ* and remote sensing observations (Key et al. 2015). GCW was established in 2011 by The Sixteenth World Meteorological Congress in Geneva. The purpose of GCW is to provide reliable information and observations on cryosphere and it's changes in a continuous basis.

According to GCW (Key et al. 2015) the amount of snow and timing of snow melt are of utmost importance for the characterization of run off. About 75% of the water supply in Western United States (Stewart et al. 2004) comes from melting snow. The importance of melt water is also big in Asia. Snow as a parameter has a big impact on transportation (aviation, trains, and vehicles), recreational activities, weather prediction and catastrophic events such as avalanches and rapid flooding. Changing snow cover has an effect on the albedo and through that to the release of greenhouse gases such as CO_2 and CH_4.

The GCW has paid attention to the fact that for snow there are a multitude of existing products and new ones being developed. The GCW emphasizes that there should be a key indicator for each geophysical parameter and thus encourages the scientific community to perform product intercomparison to recognize the assets and shortcomings of each of them. The intercomparison work is ongoing in the research community. For example, the preliminary results from ESA Satellite Snow Product Intercomparison and Evaluation Exercise (SnowPEx) (Metsämäki et al. 2016, Luojus et al. 2016) show that there is a great variety in terms of SE and SWE in the different products.

The SWE NRT product developed in this dissertation (**P. 3**) is disseminated in the original radiometer data grid, which is the EASE grid. The EASE grid is an

equal area grid, which means that even though the form of the pixel depends on latitude and longitude the area covered is constant having the value of 625 km². Since SWE describes the water layer depth of snow per unit area one can calculate easily the total snow mass from the daily SWE product. The SWE NRT data is provided for GCW in the form of SWE tracker (Key et al. 2015). This is seen as a unique product compared to the other snow indicators of GCW. One must note that mountainous regions are masked out.

The tracker displays the average snow mass for the Northern Hemisphere covering years 1982-2012. In addition, the limits for the standard deviation (±σ) are shown. The development during the current snow season is shown in red color and the last observation is marked with a black circle symbol. (Global Cryosphere Watch [ONLINE]).

The tracker thus gives an immediate insight whether the winter season under scrutiny has a total snow mass above, near or below the climatological average. The advantage is that this SWE indicator covers the Northern Hemisphere and thus better reflects the large-scale status of snow cover and is not affected much by local extremes. Mountainous regions are masked out but again, they cover a lot smaller area compared to (relatively) flat terrain.

3.4 Discussion

Both onset of snow melt and SWE have been estimated in the previous studies as described in chapter 2. However, the main scope in this research has been to enhance the detection of these parameters especially for theboreal forest zone. Most of the previously existing snow clearance day (Abdalati et al. 1995, Drobot et al. 2001, Smith et al. 1998, Mognard et al. 2003, Hall et al. 2004) and SWE products (Kelly et al. 2003, Tedesco et al. 2010) work well only on tundra or over ice. It is also noteworthy that many of the datasets made available before have a limited spatial or temporal coverage (Joshi et al. 2001, Foster et al. 2005). One of the major results in this work is thus the CDRs of snow covering the Northern Hemisphere for over three decades. Other datasets available for continental or global scale snow mass (SWE) mapping do not provide as good performance, due to the applied stand-alone satellite data retrieval methods (Kelly et al. 2003, Tedesco et al. 2010, Luojus et al. 2016). In addition, the SWE products are made available as services (GlobSnow 2018 [ONLINE], SR-SWE 2018 [ONLINE], H SAF 2018 [ONLINE]). One can obtain the daily SWE situation for both the whole Northern Hemisphere and Pan European region respectively.

The CDRs provide valuable data especially for the needs of climate research (**P. 6**). Snow clearance is known to be related to spring recovery of photosynthesis. Thus it can be used as a proxy indicator for CO_2 processes highly relevant for the carbon balance (**P. 7**). SWE mapping gives a direct measure of

snow mass over the Northern Hemisphere. Typically three decades of observational data is a minimum length for trend analyses in climate research. Such dataset is provided here for snow melt and snow mass (SWE). It is possible to use the CDRs to estimate a trend of both snow clearance date and snow mass. The CDRs can also give valuable information for the parametrization of climate models.

Knowledge on SWE is also important for the Numerical Weather Prediction (NWP) (Brasnett 1998, Pullen et al. 2011, de Rosnay et al. 2014). Since the SWE data has been made available on a daily basis as NRT services, it has the potential to be used as operational input to NWP models. However, some difficulties arise because the synoptic SD is already a part of the data assimilation and often it is preferable that such a process is performed inside the NWP algorithm. The thesis also demonstrates how the produced daily SWE information improves the hydrological river discharge forecasts (**P. 4**).

The obtained results (Fig.3) show that the snow melts now earlier than it did three decades ago. Additionally, the trend of snow mass is declining. These results are a part of a puzzle that confirms the effects of climate change at high latitudes. Discussion in public is almost exclusively concentrated on rising air temperature or declining ice sheet. It is demonstrated here that the same applies to snow mass and snow extent by using the developed methodologies. Snow is an important parameter concerning the radiation budget of the Earth. When both the snow melt takes place earlier and the total snow mass reduces it is a significant signal of climate change and also a possible source of positive feedback mechanism.

The results (**P. 7**) also demonstrate that the retrieved snow parameters can act as a proxy to higher level parameters such as SR and GPP. This can be a powerful tool to extend the spatial and temporal coverage of ground-based CO_2 flux measurements. In addition, the obtained results of the change in SR and GPP in northern boreal forests show the feasibility of the method and also make an important contribution to the climate change research.

It was shown in this work than in general the snow clearance day agrees with climate model simulation using ECHAM5 (**P. 6**). On the other hand, there are differences in regions such northern Eurasia, Taimyr Peninsula and Northern Europe. In these cases, ECHAM5 estimates the snow melt to take place too early. This behavior is also confirmed by ground reference data although the ground reference data somewhat differs from the satellite-based estimates as well. Further analysis shows that snow parameters in ECHAM5 are affected by many modelled physical processes such as large-scale circulation, temperature (snowfall in winter), computation of snow properties on ground, treatment of suface albedo, and the surface energy budget. In addition, the modelling of snow in ECHAM5 is rather simple.

The SCD dataset (**P. 2**) can be improved further by adding a quality flag to the date estimate. The time series algorithm currently produces an estimate even in suboptimal situations (shallow snowpack, wet snowpack). The algorithm now detects only SCD, where as the date of onset of snowmelt could have importance. For the analysis done in **P.7** the parameter SCD is most suitable but for the climate model (**P. 6**) additional information might be beneficial. Also, a comparison of radiometer based SCD estimates with optical FSC (Metsämäki et al. 2012) derived SCD is ongoing.

The nominal spatial resolution of available brightness temperature data has been about 25 km until recently. An enhanced dataset of brightness temperatures (Brozik et al. 2016) has been recently made available for download. This dataset contains brightness temperature fields that have been resampled with advanced methods. If the SCD and SWE CDR's are recreated using these data, the resulting CDR's would have about 5 km spatial resolution in hemispherical scale. In addition, the SR-SWE (**P.4**) approach could still be applied at least in regional scale to achieve very detailed SWE maps.

The SR-SWE (**P.4**) algorithm utilizes a forest stem volume map derived from a forest transmissivity map. These data could be applied also in hemispherical scale to get more accurate SWE retrievals. Preliminary results also show that if the forest component (Kruopis et al. 1999) of the HUT model (Pulliainen et al. 1999) is upgraded to use the approach by Cohen et al. (2015) the SWE retrieval results improve especially with deep snowpacks.

The work done in ESA SnowPEx project (Luojus et al. 2016) shows that the hemispherical SWE or snow mass estimate varies greatly depending on the type of the SWE dataset (whether it is based on model data, reanalysis of meteorological data, pure satellite product or data-assimilation product **P.3**). The SWE CDR described in **P. 3** now determines SE using dry snow algorithm (Hall et al. 2002) together with SCD algorithm (**P.2**). The estimated total snow mass might be different if another SE estimate is used. This could be important if a consensus value based on multiple data sources is required. The meteorological community would like to have (Pullen et al. 2011) the - spaceborne based component of the SWE (**P. 3**) without the synoptic SD's and the assimilation step. Thus, it might make sense to disseminate several SWE CDR's in the future and let the user select what suits their purpose best.

In the future the goal is to provide a comprehensive dataset and service that describe multiple parameters of the cryosphere. In addition to snow, the dataset could contain soil freeze and thaw (Kerr et al. 2010, Rautiainen et al. 2016) and other parameters.

4. Conclusions

In this dissertation algorithms have been developed to detect snow melt date and snow water equivalent both in hemispherical and regional scales. The main emphasis has been on developing algorithms over Northern Boreal Forests. Both parameters have been provided as CDRs over Northern Hemisphere spanning over three decades. In addition, SWE products are made available as NRT services (GlobSnow 2018 [ONLINE], SR-SWE 2018 [ONLINE], H SAF 2018 [ONLINE]).

It has also been demonstrated in this dissertation that snow melts earlier over Northern Hemisphere than it did three decades ago. Also, the snow mass has decreased during the same period. This is additional evidence for climate change. The importance is that in the public discussion the main emphasis is on temperature change and the decrease of ice sheets. Now similar evidence is provided for snow parameters of cryosphere. Snow clearance date is directly related to the CO_2 balance in the atmosphere. The dataset thus has potential to be a proxy indicator for greenhouse gases.

The CDRs also contribute to the development of climate models which is demonstrated in the publications. Using the knowledge of snow parameters in the last decades it is possible to compare the results with those provided by models. This in turn opens possibilities to enhance the models and thus obtain more accurate predictions how the climate will evolve.

Detecting SWE has also big practical importance. Hydropower plants need to know the river discharge to optimize production. In this dissertation SWE data has been used together with hydrological models. The results show that the river discharge forecasts are improved with the SWE data.

References

Abdalati, W. and Steffen, K. (1995). Passive microwave-derived snow melt regions on the Greenland ice sheet. *Geophysical Research Letters*, 22, pp. 787–790.

Armstrong, R., K. Knowles, M. Brodzik, and M. A. Hardman. (1994), updated current year. DMSP SSM/I-SSMIS Pathfinder Daily EASE-Grid Brightness Temperatures. Version 2. Boulder, Colorado USA: *NASA DAAC at the National Snow and Ice Data Center*.

Aurela, M., Laurila, T. and Tuovinen, J.P. (2004). The timing of snow melt controls the annual CO2 balance in a subarctic fen. *Geophysical Research Letters* 31, L16119, doi:10.1029/2004GL020315

Bartalev, S., D. Ershov, A. Isaev, P. Potapov, S. Turubanova, A. Yaroshenko. (2004). Russia's Forests. *TerraNorte Information System*. *RAS Space Research Institute*. (http://terranorte.iki.rssi.ru).

Betts, A. K., and Ball, J. H.(1997). Albedo over the boreal forest. *Journal of GeophysicalResearch*, 102 (D24), 28,901–28,909, doi:10.1029/96JD03876.

Bontemps, S., Defourny, P., Van Bogaert, E., Arino, O., Kalogirou, V., Ramos Perez, J. J. (2011). GLOBCOVER 2009 Products description and validation report, *Université catholique de Louvain (UCL) & European Space Agency (ESA)*, Vers. 2.2, 53 pp, hdl:10013/epic.39884.d016.

Brasnett, B. (1998). Global Analysis of Snow Depth for Numerical Weather Prediction, *Journal of Applied Meteorology*, Vol. 38, pp. 726-740.

Brodzik, M. J., D. G. Long, M. A. Hardman, A. Paget, and R. Armstrong. (2016). MEaSUREs Calibrated Enhanced-Resolution Passive Microwave Daily EASE-Grid 2.0 Brightness Temperature ESDR, Version 1. Boulder, Colorado USA. *NASA National Snow and Ice Data Center Distributed Active Archive Center*. doi: http://dx.doi.org/10.5067/MEASURES/CRYOSPHERE/NSIDC-0630.001.

Burnash, R.J.C. (1995). The NWS river forecast system—catchment modeling, In: Singh, V.P. (Ed.), Computer Models of Watershed Hydrology. *Water Resources Publications*, Littleton, Colorado, pp. 311–366.

Chang. A., Foster J., and Hall, D. (1987). Nimbus-7 SMMR derived global snow cover parameters. *Ann. Glaciol.*, 9, 39-44.

Chang. A and Tsang, L. (1992). A Neural Network Approach to Inversion of Snow Water Equivalent from Passive Microwave Measurements. *Hydrology Research*, 23 (3) 173-182.

Choudhury, B.J., Kerr, Y.H., Njoku, E.G. and Pampaloni, P. (1995). Passive Microwave Remote Sensing of Land--Atmosphere Interactions. *CRC Press*, 686 Pages ISBN 9789067641883

Cohen, J, Lemmetyinen, J, Pulliainen, J, Heinilä, K, Montomoli, F, Seppänen, J & Hallikainen, M. (2015), The Effect of Boreal Forest Canopy in Satellite Snow Mapping - A Multisensor Analysis, *IEEE Transactions on Geoscience and Remote Sensing*, , vol 53, no. 12, pp. 6593-6607.

Derksen, C. (2008). The contribution of AMSR-E 18.7 and 10.7 GHz measurements to improved boreal forest snow water equivalent retrievals. *Remote Sensing of Environment*. 112: 2700-2709.

Derksen, C., Sturm, M., Liston, G., Holmgren, J., Huntington, H., Silis, A. and Solie, D. (2009). Northwest Territories and Nunavut snow characteristics from a sub-Arctic traverse: Implications for passive microwave remote sensing. *Journal of Hydrometeorology*. 10(2): 448-463.

Déry, S. J. and Brown, R. D. (2007). Recent Northern Hemisphere snow cover extent trends and implications for the snow-albedo-feedback. *Geophys. Res. Lett.* 34, L22504.

Drobot, S.D. and Anderson, M.R. (2001).An improved method for determining snow-melt onset dates over Arctic sea ice using scanning multichannel microwave radiometer and Special Sensor Microwave/Imager data. *Journal of Geophysical Research*, 106, pp. 24–33.

Durand, M., and Margulis, S. (2006). Feasibility Test of Multifrequency Radiometric Data Assimilation to Estimate Snow Water Equivalent. *Journal of Hydrometeorology*. 7: 443-457.

Dyer, J., and Mote, T. (2006). Spatial variability and trends in observed snow depth over North America. *Geophysical Research Letters*. 33. doi:10.1029/2006GL027258.

Eagleman J.R. and Lin W.C. (1976). Remote Sensing of Soil Moisture by a 21-cm Passive Radiometer. *Journal of Geophysical Research*. vol. 81, no. 21.

Eason, R. L. (1978). Erep Sensor Systems, Skylab EREP investigations summary *NASA SP-399. Johnson Space Center*, p.343

Estilow, T. W., Young, A. H., and Robinson, D. A. (2015). A long-term Northern Hemisphere snow cover extent data record for climate studies and monitoring, *Earth Syst. Sci. Data*, 7, 137-142, https://doi.org/10.5194/essd-7-137-2015.

ETOPO5, 1990. ETOPO5 Data and Documentation | ngdc.noaa.gov. [ONLINE] Available at: https://www.ngdc.noaa.gov/mgg/global/etopo5.HTML.

Flanner, M. G., Shell, K. M., Barlage, M. , _Perovich, D. K. and Tschudi, M. A., 2011. Radiative forcing and albedo feedback from the Northern Hemisphere cryosphere between 1979 and 2008. *Nature Geoscience* 4:3, 151-155.

Foster, J. L., Sun, C. , Walker, J. P.,Kelly, R. , Chang, A., Dong J., and Powell, H. (2005). Quantifying the uncertainty in passive microwave snow water equivalent observations, *Remote Sens. Environ.* , vol. 94, no. 2, pp. 187–203.

Frei, A., Tedesco, M., Lee, S., Foster, J., Hall, D.K., Kelly, R. and Robinson, D.A. (2012). A review of global satellite-derived snow products, *Advances in Space Research*, Volume 50, Issue 8, Pages 1007-1029, ISSN 0273-1177.

GLC, 2003. Global Land Cover 2000, [ONLINE] Available at: http://forobs.jrc.ec.europa.eu/products/glc2000/glc2000.php.

Global Cryosphere Watch. 2011. Cryosphere now: snow. [ONLINE] Available at: https://globalcryospherewatch.org/state_of_cryo/snow/.

GlobLand. 2018. Copernicus Land Monitoring Service. [ONLINE] Available at: https://land.copernicus.eu/

GlobSnow, 2018. National Satellite Data Centre. [ONLINE] Available at: http://nsdc.fmi.fi/data/data_globsnow_swe.

Gloersen, P and Hardis L. (1978). The Scanning Multichannel Microwave Radiometer (SMMR) experiment. The Nimbus 7 Users' Guide. C. R. Madrid, editor. *National Aeronautics and Space Administration.* Goddard Space Flight Center, Maryland.

Groendahl, L., Friborg, T. and Soegaard, H. (2007). Temperature and snow-melt controls on interannual variability in carbon exchange in the high Arctic. *Theor. Appl. Climatol.* 88: 111. https://doi.org/10.1007/s00704-005-0228-y.

Hall, D.K., Kelly, R.E.J, Riggs, G.A, Chang, A.T.C, and Foster, J.L. (2002). Assessment of the relative accuracy of hemispheric-scale snow-cover maps. *Annals of Glaciology*, 34:24–30.

Hall, D.K., Williams, R.S, Steffen, K., Chien, J. Y. L. (2004). Analysis of Summer 2002 Melt Extent on the Greenland Sheet using MODIS and SSM/I Data. *Proceedings of IEEE International Geoscience and Remote Sensing Symposium 2004 (IGARSS)*, Anchorage, Alaska September 20-24.

Hallikainen M., Jolma P. (1992), Comparison of algorithms for retrieval of snow water equivalent from Nimbus-7 SMMR data in Finland. *IEEE Transactions on Geoscience and Remote Sensing*, Vol. 30, 124-131.

Haykin, S. (1999). Neural Networks, a Comprehensive Foundation 2. ed. *Prentice Hall.*

H SAF, 2018. H-SAF Official Web Site. [ONLINE] Available at: http://hsaf.meteoam.it/.

Imaoka, K., Kachi, M., Fujii, H., Murakami, H., Hori, M., Ono, A., Igarashi, T., Nakagawa, K., Oki, T., Honda, Y., Shimoda, H. (2010). Global Change Observation Mission (GCOM) for monitoring carbon, water cycles, and climate change. *Proc. of the IEEE*, 98, pp 717-734.

Joshi M., Merry C.J., Jezek, K.C. and Bolzan, J.F. (2001). An edge detection technique to estimate melt duration, season and melt extent on the Greenland ice sheet using passive microwave data. *Geophysical Research Letters*, 28, pp. 3497.

Kawanishi, T., Sezai, T., Ito Y., Imaoka, K., Takeshima T., Ishido Y., Shibata, A., Miura,M. Inahata, H., Spencer, R.W. (2003). The Advanced Microwave Scanning Radiometer for the Earth Observing System (AMSR-E), NASDA's contribution to the EOS for global energy and water cycle studies. *IEEE Transactions on Geoscience and Remote Sensing*, vol. 41, no. 2, pp. 184-194, Feb. 2003. doi: 10.1109/TGRS.2002.808331

Kelly, R., Chang, A., Tsang, L. and Foster, J. (2003). A prototype AMSR-E global snow area and snow depth algorithm. *IEEE Transactions on Geoscience and Remote Sensing*. 41(2): 230-242.

Kerr, Y. H., Waldteufel, P., Wigneron, J-P., Delwart, S., Cabot, F., Boutin, J., Escorihuela, M-J., Font, J., Reul, N., Gruhier, C., Juglea, S. E., Drinkwater, M. R., Hahne, A., Martin-Neira, M. and Mecklenburg, S. (2010). The SMOS mission: New tool for monitoring key elements of the global water cycle, *Proc. IEEE*, 98(5), 666–687, doi:10.1109/JPROC.2010.2043032.

Key, K., Goodison, B., Schöner, W., Godøy, Ø., Ondráš, M. and Snorrason, Á. A Global Cryosphere Watch. (2015). *Arctic*, vol 68, no 5, p. 48-58. doi:10.14430/arctic4476.

Kitaev, L., Kislov. A, Krenke, A., Razuvaev, V., Martuganov, R. and Konstantinov, I. (2002). The snow characteristics of northern Eurasia and their relationship to climatic parameters. *Boreal Environment Research* 7:437-445.

Knowles, K., E. Njoku, R. Armstrong, and M.J. Brodzik. (2002). Nimbus-7 SMMR Pathfinder daily EASE-Grid brightness temperatures. Boulder, CO: *National Snow and Ice Data Center*. Digital media and CD-ROM.

Kohonen, T. (1982). Self-organized formation of topologically correct feature maps. *Biol. Cybern*. 43: 59. https://doi.org/10.1007/BF00337288

Kruopis, N., Praks, J., Arslan, A., Alasalmi, H., Koskinen, J., andHallikainen, M. (1999).Passive microwave measurements of snow-covered forests in EMAC'95. *IEEE Transactions on Geoscience and Remote Sensing*, 37 ,2699–2705.

Kuusisto, E. (1984). Snow accumulation and snowmelt in Finland, *Helsinki: Water Research Institute*, no. 55.

Luojus, K., Pulliainen, J., Cohen, J., Ikonen, J., Derksen, C., Mudryk, L., Nagler, T. and Bojkov, B. (2016). Assessment of Northern Hemisphere Snow Water Equivalent Datasets in ESA SnowPEx project, *EGU General Assembly 2016*, held 17-22 April, 2016 in Vienna Austria, id. EPSC2016-2941.

Macelloni, G., Brogioni, M., Montomoli, F., Lemmetyinen, J., Pulliainen, J. and Rott, H. (2014). Retrieval of snow water equivalent in forested area using multifrequency SAR data, *EUSAR 2014; 10th European Conference on Synthetic Aperture Radar*, Berlin, Germany, pp. 1-3.

Metsämäki, S., Mattila, O-P., Pulliainen, J., Niemi, K., Luojus, K. and Böttcher, K. (2012). An optical reflectance model-based method for fractional snow cover mapping applicable to continental scale, *Remote Sensing of Environment*, Volume 123, Pages 508-521, ISSN 0034-4257, https://doi.org/10.1016/j.rse.2012.04.010.

Metsämäki, S., Pulliainen, J., Salminen, M., Luojus, K., Wiesmann, A., Solberg, R., Böttcher, K., Hiltunen, M. and Ripper, E. (2015). Introduction to GlobSnow Snow Extent products with considerations for accuracy assessment, *Remote Sensing of Environment*, Volume 156, Pages 96-108, ISSN 0034-4257, https://doi.org/10.1016/j.rse.2014.09.018.

Metsämäki, S., Ripper, E., Mattila O-P., Fernandes, R., Bippus, G., Luojus, K., Nagler, T., and Bojkov, B. (2016). Evaluation of Northern Hemisphere Snow Extent products within ESA SnowPEx-project, *2016 IEEE International Geoscience and Remote Sensing Symposium (IGARSS)*, Beijing, pp. 5280-5283.doi: 10.1109/IGARSS.2016.7730375

Mognard, N.M., Kouraev, A.V., Josberger, E.G. (2003). Global Snow-Cover Evolution from Twenty Years of Satellite Passive Microwave Data. *Proceedings of IEEE International Geoscience and Remote Sensing Symposium 2003 (IGARSS)*, Toulouse, France July 21-25, 2003. Available electronically via http://ieeexplore.ieee.org.

National Ice Center. (2008), updated daily. IMS Daily Northern Hemisphere Snow and Ice Analysis at 1 km, 4 km, and 24 km Resolutions, Version 1. [4 km version]. Boulder, Colorado USA. NSIDC: National Snow and Ice Data Center. doi: http://dx.doi.org/10.7265/N52R3PMC.

Oudin, L., Hervieu, F., Michel, C., Perrin, C., Andreassian V., Anctil, F., Loumagne, C. (2004). Which potential evapotranspiration input for a lumpedrainfall–runoff model? Part 2 Towards a simple and efficient potential evapotranspiration model for rainfall–runoff modelling, *Journal of Hydrology* 303, pp. 290-306.

Pullen, S., Jones, C. and Rooney, G. (2011). Using Satellite-Derived Snow Cover Data to Implement a Snow Analysis in the Met Office Global NWP Model. *Journal of Applied Meteorology and Climatology*, vol. 50, pp. 958-973.

Pulliainen, J., Grandell J. and Hallikainen, M. (1999). HUT snow emission model and its applicability to snow water equivalent retrieval, *IEEE Transactions on Geoscience and Remote Sensing*, vol. 37, no. 3, pp. 1378-1390, May. doi: 10.1109/36.763302

Pulliainen, J. (2006). Mapping of snow water equivalent and snow depth in boreal and sub-arctic zones by assimilating space-borne microwave radiometer data and ground-based observations. *Remote Sensing of Environment*, 101, 257-269.

Ramage, J. M., and Isacks, B. L. (2002). Determination of melt-onset and refreeze timing on southeast Alaskan icefields usingSSM/I diurnal amplitude variations,Annals of Glaciology 34, 391–398, doi:10.3189/172756402781817761.

Rautiainen, K., Parkkinen, T., Lemmetyinen, J., Schwank, M. Wiesmann, A., Ikonen, J., Derksen, C., Davydov, S., Davydova, A., Boike, J., Langer, M., Drusch, M. and

Pulliainen, J. (2016). SMOS prototype algorithm for detecting autumn soil freezing. *Remote Sensing of Environment*, 180, 346-360.

Riihelä, A. (2013). The Surface Albedo of the Arctic from Spaceborne Optical Imagers: Retrieval and Validation. Dissertation, *Finnish Meteorological Institute Contributions*, 101.

de Rosnay, P., Balsamo, G., Albergel, C., Muñoz-Sabater, J. and Isaksen L. (2014). Initialisation of Land Surface Variables for Numerical Weather Prediction. *Surv. Geophys.*, 35: 607. https://doi.org/10.1007/s10712-012-9207-x

Saberi, N. , Kelly, R. , Toose, P. , Roy, A. and Derksen, C. (2017). Modeling the Observed Microwave Emission from Shallow Multi-Layer Tundra Snow Using DMRT-ML. *Remote Sensing*, 9, 1327. doi:10.3390/rs9121327

Simpson, J.J. and McIntire T.J. (2001). A Recurrent Neural Network Classifier for Improved Retrievals of Areal Extent of Snow Cover. *IEEE Transactions on Geoscience and Remote Sensing*, 39, 10, Oct.

Smith, D. M. (1998). Observation of perennial Arctic sea ice melt and freeze-up using passive microwave data. *Journal Geophysical Research*, 103(C12), pp. 27753–27769.

Smith, N.V., Saatchi, S.S. and Randerson, J.T. (2004). Trends in northern latitude soil freeze and thaw cycles from 1988 to 2002, *Journal of geophysical research*, 109.

SR-SWE, 2018. National Satellite Data Centre. [ONLINE] Available at: http://nsdc.fmi.fi/data/data_super_swe.

Stewart, I.T., Cayan, D.R. and Dettinger, M.D. (2004). Changes in snowmelt runoff timing in western North America under a 'business as usual' climate change scenario. *Climatic Change* 62(1-3):217 – 232.

Sturm, M. Taras, B, Liston,G., Derksen, C., Jonas, T. and Lea ,J. (2010). Estimating snow water equivalent using snow depth data and climate classes. *Journal of Hydrometeorology*. 11: 1380-1394.

Tao H., Shunlin, L. and Song, D-X. (2014). Analysis of global land surface albedo climatology and spatial-temporal variation during 1981-2010 from multiple satellite products. *Journal of Geophysical Research: Atmospheres* 119:17, 10,281-10,298.

Tedesco, M. and Narvekar, P. S. (2010). Assessment of the NASA AMSR-E SWE Product, *IEEE Journal of Selected Topics in Applied Earth Observations and Remote Sensing*, vol. 3, no. 1, pp. 141-159, March. doi: 10.1109/JSTARS.2010.2040462

Tiuri, M. E., Sihvola, A. H., Nyfors E. G. and Hallikainen, M. T. (1984). The complex dielectric constant of snow at microwave frequencies. *IEEE J. Oceanic Eng.,* 9(5), 377–382.

Ulaby, F. T., Moore, R. K. and Fung, A. K.. (1981). Microwave Remote Sensing: Active and Passive, Vol. I -- Microwave Remote Sensing Fundamentals and Radiometry, *Addison-Wesley, Advanced Book Program,* Reading, Massachusetts, 456 pages.

Wiesmann, A., and Matzler, C. (1999): Microwave emission model of layered snowpacks. *Remote Sens. Environ.*, 70, 307-316.

Wilheit, T. (1972), The Electrically Scanning Microwave Radiometer (ESMR) Experiment, *Nimbus-5 User's Guide*, NASA/Goddard Space Flight Center, Greenbelt, Maryland, 59–105.

Winchell, T. S., Barnard, D. M. , Monson, R. K. , Burns, S. P. and Molotch, N. P. (2016). Earlier snowmelt reduces atmospheric carbon uptake in midlatitude

subalpine forests, *Geophys. Res. Lett.,* 43, 8160–8168, doi:10.1002/2016GL069769.

Yang H., Weng, F., Lv, L., Lu, N., Liu, G., Bai, M., Qian, Q., He, J. and Xu, H. (2011). The FengYun-3 Microwave Radiation Imager On-Orbit Verification, *IEEE Transactions on Geoscience and Remote Sensing*, vol. 49, no. 11, pp. 4552-4560,doi: 10.1109/TGRS.2011.2148200

Zhou, H., Aizen, E. and Aizen, V. (2013). Deriving long term snow cover extent dataset from AVHRR and MODIS data: Central Asia case study, *Remote Sensing of Environment*, Volume 136, Pages 146-162, ISSN 0034-4257, https://doi.org/10.1016/j.rse.2013.04.015.

FINNISH METEOROLOGICAL INSTITUTE
Erik Palménin aukio 1
P.O. Box 503
FI-00101 HELSINKI
tel. +358 29 539 1000
WWW.FMI.FI

FINNISH METEOROLOGICAL INSTITUTE
CONTRIBUTIONS No. 151
ISBN 978-952-336-065-5 (pdf)
ISSN 0782-6117
Helsinki 2018